Received: 10 July 2017 | Revised: 15 September 2017 | Accepted: 21 September 2017
DOI: 10.1002/bit.26459

ARTICLE

WILEY BIOTECHNOLOGY & BIOENGINEERING

Engineering of cell membrane to enhance heterologous production of hyaluronic acid in *Bacillus subtilis*

Adam W. Westbrook | **Xiang Ren** | **Murray Moo-Young** | **C. Perry Chou**

Department of Chemical Engineering, University of Waterloo, Waterloo, Ontario, Canada

Correspondence
C. Perry Chou, Department of Chemical Engineering, University of Waterloo, Waterloo, Ontario, Canada, N2L 5B6.
Email: cpchou@uwaterloo.ca

Funding information
Natural Sciences and Engineering Research Council of Canada, Grant number: 950-211471

Abstract

Hyaluronic acid (HA) is a high-value biopolymer used in the biomedical, pharmaceutical, cosmetic, and food industries. Current methods of HA production, including extraction from animal sources and streptococcal cultivations, are associated with high costs and health risks. Accordingly, the development of bioprocesses for HA production centered on robust "Generally Recognized as Safe (GRAS)" organisms such as *Bacillus subtilis* is highly attractive. Here, we report the development of novel strains of *B. subtilis* in which the membrane cardiolipin (CL) content and distribution has been engineered to enhance the functional expression of heterologously expressed hyaluronan synthase (HAS) of *Streptococcus equisimilis* (SeHAS), in turn, improving the culture performance for HA production. Elevation of membrane CL levels via overexpressing components involved in the CL biosynthesis pathway, and redistribution of CL along the lateral membrane via repression of the cell division initiator protein FtsZ resulted in increases to the HA titer of up to 204% and peak molecular weight of up to 2.2 MDa. Moreover, removal of phosphatidylethanolamine and neutral glycolipids from the membrane of HA-producing *B. subtilis* via inactivation of *pssA* and *ugtP*, respectively, has suggested the lipid dependence for functional expression of SeHAS. Our study demonstrates successful application of membrane engineering strategies to develop an effective platform for biomanufacturing of HA with *B. subtilis* strains expressing Class I streptococcal HAS.

KEYWORDS
Bacillus subtilis, CRISPR, hyaluronan, hyaluronic acid, membrane engineering, transcriptional interference

1 | INTRODUCTION

Hyaluronic acid (HA) is a high-value biopolymer used in a broad range of applications such as abdominal, pelvic, and opthalmic surgeries; viscosupplement injections for osteoarthritis treatment; and various health, food, and cosmetic products (Goa & Benfield, 1994; Liu, Liu, Li, Du, & Chen, 2011). The current US market for HA is estimated to exceed $1 billion annually and is expected to increase quickly due to the escalating demand for viscosupplements and dermal fillers (Liu et al., 2011). HA is a linear and unbranched polysaccharide composed of alternating *N*-acetyl-glucosamine (GlcNAc) and glucuronic acid (GlcUA) monomers, and can reach 8 MDa in size (Widner et al., 2005). High-molecular-weight (MW) HA possesses an enhanced capacity to retain water, a desirable characteristic for biomedical applications (Chong, Blank, McLaughlin, & Nielsen, 2005). In the past, HA was extracted primarily from rooster combs, but the high cost of purification, limited availability, and concerns regarding allergic reactions or viral infections resulting from exposure to contaminated preparations created interest in alternative methods for HA production (O'Regan, Martini, Crescenzi, De Luca, & Lansing, 1994;

Pullman-Mooar, Mooar, Sieck, Clayburne, & Schumacher, 2002). Microbial HA synthesis via attenuated strains of group C streptococci (i.e., *Streptococcus equisimilis* and *Streptococcus zooepidemicus*) has gradually replaced extraction from animal tissues, and is currently the dominant method of industrial HA production (Liu et al., 2011). However, HA produced from *Streptococcus* sp. may contain exotoxins inherent to these pathogenic species (Widner et al., 2005), and the fastidious nature of these organisms increases manufacturing costs (Vázquez, Montemayor, Fraguas, & Murado, 2010). Accordingly, the adoption of robust nonpathogenic bacteria as HA production hosts has garnered much attention in recent years (Liu et al., 2011). *Bacillus subtilis* is a genetically tractable model Gram-positive microorganism, grows rapidly in simple medium, has been granted a "Generally Recognized as Safe (GRAS)" designation by the Food and Drug Administration (Schallmey, Singh, & Ward, 2004), and, therefore, can be an ideal host for HA production. Noticeably, high-level production of HA has been demonstrated in *B. subtilis* on an industrial scale (Liu et al., 2011).

HA is naturally synthesized by certain pathogenic strains of bacteria, such as Lancefield group A (DeAngelis, Papaconstantinou, & Weigel, 1993) and C (Kumari & Weigel, 1997) streptococci, and Type A *Pasteurella multocida* (DeAngelis, Jing, Drake, & Achyuthan, 1998), as a means of evading the host immune response (Weigel & DeAngelis, 2007). The hyaluronan synthase (HAS) autonomously synthesizes HA from uridine diphosphate (UDP)-GlcNAc and UDP-GlcUA, and is classified as either a Class I or II HAS based on topology (i.e., transmembrane and peripheral membrane proteins for Class I and II HAS, respectively) and the number of glycosyltransferase 2 family modules present (i.e., one and two modules for Class I and II HAS, respectively). The relatively small size and few transmembrane domains of streptococcal HAS suggest that they cannot facilitate pore formation for translocation of the growing HA chain (Weigel, 2002). This theory was supported by the observation that mutation of a component of an ABC transporter complex reduced HA capsule size in *Streptococcus pyogenes*, suggesting that additional proteins may assist translocation (Ouskova, Spellerberg, & Prehm, 2004). However, recent work showed that HAS derived from *S. equisimilis* (SeHAS; encoded by *seHas*) could mediate the release of the small fluorescent dye Cascade Blue from inside liposomes, and that mutations, which decreased HAS activity and HA MW in an earlier study, in one of its transmembrane domains resulted in reduced Cascade Blue efflux (Kumari, Baggenstoss, Parker, & Weigel, 2006; Medina, Lin, & Weigel, 2012). Similarly, purified SeHAS, reconstituted into *Escherichia-coli*-derived or synthetic proteoliposomes, synthesized and translocated high MW HA into the vesicle lumen, requiring only exogenous UDP-GlcUA and UDP-GlcNAc (Hubbard, McNamara, Azumaya, Patel, & Zimmer, 2012). These observations, along with the demonstration of HA production in a variety of bacteria heterologously expressing HAS (Chien & Lee, 2007b; Mao, Shin, & Chen, 2009; Widner et al., 2005; Yoshimura, Shibata, Hamano, & Yamanaka, 2015), indicate that a single HAS protein produces HA autonomously via a process requiring as many as seven different functions to initiate and elongate the HA chain, and extrude it across the membrane (Weigel, 2002).

Over the past decade, engineering of *B. subtilis* for heterologous production of HA has been explored. In an early demonstration, it was shown that UDP-GlcUA is limiting for HA synthesis, which can be enhanced by coexpression of *tuaD* (encoding native UDP-glucose-6 dehydrogenase; TuaD) and *seHas*. Coexpression of additional native enzymes involved in the HA biosynthetic pathway, that is uridine triphosphate (UTP)-glucose-1-P uridylyltransferase (GtaB; encoded by *gtaB*) and UDP-GlcNAc pyrophosphorylase (GcaD; encoded by *gcaD*), provided moderate improvements to the HA titer (Widner et al., 2005). Coexpression of *szHas* (encoding HAS from *S. zooepidemicus*; SzHAS), *tuaD*, and *vhb* (encoding hemoglobin from *Vitreoscilla*; VHb), significantly increased the HA titer presumably due to increased ATP availability resulting from *vhb* expression (Chien & Lee, 2007a). A recent study revealed the effects of overexpressing various combinations of genes involved in the HA biosynthetic pathway, including *szHas*, *tuaD*, *gtaB*, *gcaD*, *glmS* (encoding native L-glutamine-D-fructose-6-phosphate amidotransferase; GlmS), and *glmM* (encoding native phosphoglucosamine mutase; GlmM), as well as downregulating expression of *pfkA* (encoding 6-phosphofructokinase; PfkA) on HA MW and titer (Jin, Kang, Yuan, Du, & Chen, 2016). A strain coexpressing *szHas*, *tuaD*, *gtaB*, *glmS*, *glmM*, and *gcaD* produced ~30% more HA than strains coexpressing only *szHas* and *tuaD*, or *szHas* and *gcaD*, while the MW was not improved. On the other hand, simply downregulating expression of *pfkA*, via replacement of the native ATG start codon with TTG, improved the HA titer by 18% (Jin et al., 2016). Moreover, the carbon source used to produce HA in *B. subtilis* cultures can affect the MW profile (Westbrook, Moo-Young, & Chou, 2016).

Cardiolipin (CL) is the least abundant phospholipid present in the membrane of growing *B. subtilis* cells as a dimer of the essential and abundant anionic phospholipid phosphatidylglycerol (PG) (Kawai, Hara, Takamatsu, Watabe, & Matsumoto, 2006; Salzberg & Helmann, 2008). PG is synthesized from cytosine diphosphate (CDP)-diacylglycerol by phosphatidylglycerophosphate synthase (PgsA; encoded by *pgsA*), and CL is subsequently produced from PG by the major CL synthase (ClsA; encoded by *clsA*) (Salzberg & Helmann, 2008). ClsA localizes at the septal region of the *B. subtilis* membrane in a FtsZ-dependent manner (Note that FtsZ initiates cell division.), presumably to assist in the assembly of the cell division machinery (Kawai et al., 2004). FtsZ depletion potentially results in dispersion of ClsA along the lateral membrane and, in turn, spatially coupled dispersion of CL (Nishibori, Kusaka, Hara, Umeda, & Matsumoto, 2005). The dependence of Class I HAS activity on its orientation with CL was first observed when the activity of the solubilized HAS of *S. pyogenes* (SpHAS) was recovered upon treatment with CL (Triscott & van de Rijn, 1986). Active SpHAS and SeHAS were observed to be ~23 kDa larger than the purified enzymes, both of which were inactive (Tlapak-Simmons, Kempner, Baggenstoss, & Weigel, 1998). Furthermore, the activity of purified SpHAS was not significantly enhanced by other lipids in vitro, and although the in vitro activity of purified SeHAS was stimulated by phosphatidic acid (PA) and phosphatidylserine, CL provided the greatest enhancements to SeHAS activity (Tlapak-Simmons, Baggenstoss, Clyne, & Weigel, 1999). Therefore, it was proposed that ~16 CL molecules interact with a single SpHAS or SeHAS protein, and that loss of even a single molecule can cause

enzyme inactivation. Accordingly, CL may assist HAS in creating an internal pore-like passage for HA translocation (Tlapak-Simmons et al., 1998), which is similar to the function of CL proposed for several mitochondrial membrane proteins that lack transport capability in its absence (Dowhan, 1997). In addition, interactions between CL and HA may add to the net retention force that keeps the HA-UDP/HAS complex together during polymerization until a sufficient opposing (release) force exceeds the net retention force, resulting in the release (and cessation of growth) of the growing HA chain (Tlapak-Simmons et al., 1999; Weigel & Baggenstoss, 2012).

While membrane engineering for enhanced biological production is a challenging strategy with increasing applications in bacteria (Chen, 2007; Chou, 2007), the approach is unpopular for *B. subtilis*. A documented study focused on the alteration of the lipid composition of the *B. subtilis* membrane, leading to enhanced secretion of the industrially important enzyme α-amylase (Cao, Heel, Ahmed, Mols, & Kuipers, 2017). Mutation of *clsA* or *pssA*, encoding phosphatidylserine synthase (PssA), significantly increased extracellular amylase production, presumably through creating a more negative membrane charge density (Cao et al., 2017). In this study, we engineered the cell membrane of an HA-producing strain of *B. subtilis* to increase the functional expression of heterologously expressed SeHAS and, in turn, improve HA production. The membrane CL content was increased by overexpressing *pgsA* and *clsA*, resulting in significant improvements to the HA titer and MW. To further enhance the functional expression of SeHAS, we then altered the distribution of CL in the membrane by reducing the expression of *ftsZ* via CRISPR interference (CRISPRi) using our recently developed CRISPR-Cas9 toolkit for *B. subtilis* (Westbrook et al., 2016). The reduced *ftsZ* expression led to partial redistribution of CL along the lateral membrane and, as a result, improved HA titers and MWs in shake flask cultures. We also assessed the efficacy of increasing dCas9 expression to modulate targeted gene expression. The results of this study have shed new light on the lipid dependence for functional expression of streptococcal Class I HAS in *B. subtilis*.

2 | MATERIALS AND METHODS

2.1 | Bacterial strains, primers, and plasmids

The *B. subtilis* strains used in this study are listed in Table 1. *E. coli* HI-Control™ 10G chemically competent cells (Lucigen; WI) were prepared to be electrocompetent as described previously (Sambrook & Russell, 2001) and used as host for molecular cloning and plasmid construction. *B. subtilis* and *E. coli* strains were maintained as glycerol stocks stored at −80°C. Primers (Table 1) were synthesized by Integrated DNA Technologies (IDT; IA).

2.2 | Plasmid construction and transformation

DNA manipulation was performed using standard molecular cloning techniques (Sambrook & Russell, 2001), and DNA sequencing was conducted by The Center for Applied Genomics (TCAG; ON). To construct an expression cassette in which *pgsA* and *clsA* were driven by the strong promoter P_{grac}, *pgsA*, and *clsA* were amplified by polymerase chain reaction (PCR) with respective primers P122/P123 and P124/P125 from 1A751 genomic DNA (gDNA), and the two fragments were spliced via Splicing by Overlap Extension (SOE)-PCR (this process is subsequently referred to as "splicing"). The spliced fragment was then inserted into BamHI/SpeI-digested pAW005, yielding pAW001-4. pAW005 is a pHT01 (Nguyen, Phan, & Schumann, 2007) derivative containing a multiple cloning site (MCS) comprised of BamHI-AatII-SbfI-AscI and SpeI-NgoMIV-NotI-AsiSI-AgeI-XmaI restriction sites flanking promoter $P_{grac.max}$, a modified version of P_{grac} (i.e., promoter P01) (Phan, Nguyen, & Schumann, 2012). The MCS was synthesized by Bio Basic (Ontario, Canada) and the sequence is provided in Table 1. $P_{grac.max}$ contains the upstream promoter element (UP) of promoter P64, the −35 region of promoter P71, the −15 region of promoter P57, the native −10 region, and a T-C substitution at the +3 site (Phan et al., 2012). pAW005 was constructed by amplifying the synthesized MCS with primers P126/P127, followed by insertion into BamHI/XmaI-digested pHT01. The P_{grac}::*pgsA*:*clsA* cassette, including the partial MCS and *trpA* terminator from *E. coli*, was amplified with primers P128/P129 from pAW001-4, and the *thrC* 5′- homology length (HL-5′) was amplified with primers P130/P131 from 1A751 gDNA, and the two fragments were spliced, generating a *thrC* HL-5′-P_{grac}::*pgsA*:*clsA* cassette. This cassette was inserted into SbfI/NheI-digested pAW004-2 (Westbrook et al., 2016), yielding pAW002-4. Plasmid pAW003-4 is similar to pAW002-4 but contains promoter $P_{grac.UPmod}$, that is promoter P61 which is a weaker derivative of promoter P_{grac}, in place of promoter P_{grac}. It was constructed from pAW001-4 in the same way as pAW002-4, except that primers P132 and P133 were used in place of primers P128 and P131, respectively. The gRNA cassettes *ftsZ*-gRNA.P79NT, *ftsZ*-gRNA.P79NT(10A-G), *ftsZ*-gRNA.P79NT(15C-U), *ftsZ*-gRNA.P244NT, *ftsZ*-gRNA.P244NT(15C-A), and *ftsZ*-gRNA.P533NT were amplified with respective forward primers P134-P139 and a common reverse primer P32 from pgRNA-bacteria (Qi et al., 2013), and inserted into SphI/NcoI-digested pAW017-2 (Westbrook et al., 2016) to obtain respective gRNA delivery vectors pAW004-4, pAW005-4, pAW006-4, pAW007-4, pAW008-4, and pAW009-4. All gRNA delivery vectors were linearized with SacI prior to transformation. To construct the integration vector for mutation of *pssA*, the *pssA* HL-5′, and HL-3′ were amplified from 1A751 gDNA with respective primers P140/P141 and P142/P143, followed by sequential insertion in place of the corresponding *thrC* HL-5′ and HL-3′ of pAW004-2 using the respective SbfI/NheI and AscI/AgeI restriction sites, yielding pAW010-4. pAW011-4, an integration vector for mutation of *ugtP*, was constructed in the same way as pAW010-4, except the *ugtP* HL-5′ and HL-3′ were amplified with primers P144/P145 and P146/P147. Competent cell preparation and transformation, and eviction of the P_{araE}::*mazF*-Spc^R cassette after transformation of counter-selectable integration vectors were performed as previously described (Westbrook et al., 2016).

TABLE 1 Strains, plasmids, and primers used in this study

Strain or plasmid	Characteristics[a]	Source
E. coli HI-Control™ 10G	*mcrA Δ(mrr-hsdRMS-mcrBC) endA1 recA1* φ80d*lacZ*ΔM15 Δ*lacX74 araD139* Δ (*ara,leu*)7697*galU galKrpsL* (StrR) *nupG* λ− *tonA* Mini-F *lacIq1* (Gent^R)	Lucigen
B. subtilis		
168/1A1	*trpC2*	Burkholder and Giles (1947)
1A786	*amyE*::*cat* Cm lacA::*spec leuB8 metA4* Sp *hsd*(*Rl*)R+M-	Härtl, Wehrl, Wiegert, Homuth, Schumann (2001)
1A751	*his nprR2 nprE18 ΔaprA3 ΔeglS102 ΔbglTbglSRV*	Wolf et al. (1995)
AW008	1A751 *amyE*::(P_{grac}::*seHas*:*tuaD*, Neo^R)	This work
AW001-4	1A751 *amyE*::(P_{grac}::*seHas*:*tuaD*, Neo^R), *thrC*::(P_{grac}::*pgsA*:*clsA*)	This work
AW002-4	1A751 *amyE*::(P_{grac}::*seHas*:*tuaD*, Neo^R), *lacA*::($P_{xylA,\ Bm}$::d*cas9*,*xylR*, Erm^R)	This work
AW003-4	1A751 *amyE*::(P_{grac}::*seHas*:*tuaD*, Neo^R), *lacA*::($P_{xylA,\ Bm}$::d*cas9*,*xylR*, Erm^R), *thrC*::(P_{grac}::*pgsA*:*clsA*)	This work
AW004-4	1A751 amyE::(*P_{grac}*::*seHas*:*tuaD*, *Neo^R*), *lacA*::(*P_{xylA}*, Bm::*dcas9*,*xylR*, *Erm^R*), *thrC*::(*P_{grac}*::*pgsA*:*clsA*), *wprA*::(*$P_{xylA.SphI+1}$*::*ftsZ*-gRNA.P79NT(15C-U))	This work
AW005-4	1A751 *amyE*::(P_{grac}::*seHas*:*tuaD*, Neo^R), *lacA*::($P_{xylA,\ Bm}$::d*cas9*,*xylR*, Erm^R), *wprA*::($P_{xylA.SphI+1}$::*ftsZ*-gRNA.P79NT(15C-U))	This work
AW006-4	1A751 *amyE*::(P_{grac}::*seHas*:*tuaD*, Neo^R), *lacA*::($P_{xylA,\ Bm}$::d*cas9*,*xylR*, Erm^R), *wprA*::($P_{xylA.SphI+1}$::*ftsZ*-gRNA.P244NT)	This work
AW007-4	1A751 *amyE*::(P_{grac}::*seHas*:*tuaD*, Neo^R), *lacA*::($P_{xylA,\ Bm}$::d*cas9*,*xylR*, Erm^R), *thrC*::($P_{grac.UPmod}$::*pgsA*:*clsA*)	This work
AW008-4	1A751 *amyE*::(P_{grac}::*seHas*:*tuaD*, Neo^R), *lacA*::($P_{xylA,\ Bm}$::d*cas9*,*xylR*, Erm^R), *thrC*::($P_{grac.UPmod}$::*pgsA*:*clsA*), *wprA*::($P_{xylA.SphI+1}$::*ftsZ*-gRNA.P79NT(15C-U))	This work
AW009-4	1A751 *amyE*::(P_{grac}::*seHas*:*tuaD*, Neo^R), *lacA*::($P_{xylA,\ Bm}$::dcas9,xylR, Erm^R), *thrC*::($P_{grac.UPmod}$::*pgsA*:*clsA*), *wprA*::($P_{xylA.SphI+1}$::*ftsZ*-gRNA.P244NT)	This work
AW010-4	1A751 *amyE*::(P_{grac}::*seHas*:*tuaD*, Neo^R), *lacA*::($P_{xylA,\ Bm}$::d*cas9*,*xylR*, Erm^R), *thrC*::($P_{grac.UPmod}$::*pgsA*:*clsA*), *wprA*::($P_{xylA.SphI+1}$::*ftsZ*-gRNA.P244NT(15C-A))	This work
AW011-4	1A751 *amyE*::(P_{grac}::*seHas*:*tuaD*, Neo^R), *lacA*::($P_{xylA,\ Bm}$::d*cas9*,*xylR*, Erm^R), *thrC*::($P_{grac.UPmod}$::*pgsA*:*clsA*), *wprA*::($P_{xylA.SphI+1}$::*ftsZ*-gRNA.P533NT)	This work
AW012-4	1A751 *amyE*::(P_{grac}::*seHas*:*tuaD*, Neo^R), Δ*pssA*	This work
AW013-4	1A751 *amyE*::(P_{grac}::*seHas*:*tuaD*, Neo^R), Δ*ugtP*	This work
Plasmids		
pAW004-2	P_{araE}::*mazF*, *araR*,Spc^R, Erm^R, *B. subtilis* auto-evicting counter-selectable *thrC* integration vector	Westbrook et al. (2016)
pAW017-2	$P_{xylA.SphI+1}$,P_{araE}::*mazF*, *araR*,Spc^R, Erm^R, *B. subtilis* auto-evicting counter-selectable *wprA* integration vector	Westbrook et al. (2016)
pAW019-2	$P_{xylA,Bm}$::*dcas9*, *xylR*, Amp^R, Erm^R, *B. subtilis lacA* integration vector	Westbrook et al. (2016)
pAW005	*lacI*, P_{grac}, MCS, Cat^R, Amp^R, B. *subtilis* replicating shuttle vector	This work
pAW008	P_{grac}::*seHas*:*tuaD*, Neo^R, Amp^R, *B. subtilis amyE* integration vector	Westbrook et al. (2016)
pAW001-4	*lacI*, P_{grac}::*pgsA*:*clsA*, MCS, Cat^R, Amp^R, *B. subtilis* replicating shuttle vector	This work
pAW002-4	P_{grac}::*pgsA*:*clsA*, P_{araE}::*mazF*, *araR*,Spc^R, Erm^R, *B. subtilis* auto-evicting counter-selectable *thrC* integration vector	This work
pAW003-4	$P_{grac.UPmod}$::*pgsA*:*clsA*, P_{araE}::*mazF*, *araR*, Spc^R, Erm^R, *B. subtilis* auto-evicting counter-selectable *thrC* integration vector	This work
pAW004-4	$P_{xylA.SphI+1}$::*ftsZ*-gRNA.P79NT,P_{araE}::*mazF*, *araR*, Spc^R, Erm^R, *B. subtilis* auto-evicting counter-selectable *wprA* integration vector	This work
pAW005-4	$P_{xylA.SphI+1}$::*ftsZ*-gRNA.P79NT(10A-G), P_{araE}::*mazF*, *araR*, Spc^R, Erm^R, *B. subtilis* auto-evicting counter-selectable *wprA* integration vector	This work
pAW006-4	$P_{xylA.SphI+1}$::*ftsZ*-gRNA.P79NT(15C-U), P_{araE}::*mazF*, *araR*, Spc^R, Erm^R, *B. subtilis* auto-evicting counter-selectable *wprA* integration vector	This work
pAW007-4	$P_{xylA.SphI+1}$::*ftsZ*-gRNA.P244NT, P_{araE}::*mazF*, *araR*, Spc^R, Erm^R, *B. subtilis* auto-evicting counter-selectable *wprA* integration vector	This work

(Continues)

TABLE 1 (Continued)

Strain or plasmid	Characteristics[a]	Source
pAW008-4	$P_{xylA.SphI+1}$::*ftsZ*-gRNA.P244NT(15C-A), P_{araE}::*mazF*, *araR*, Spc^R, Erm^R, *B. subtilis* auto-evicting counter-selectable wprA integration vector	This work
pAW009-4	$P_{xylA.SphI+1}$::*ftsZ*-gRNA.P533NT, P_{araE}::*mazF*, *araR*, Spc^R, Erm^R, *B. subtilis* auto-evicting counter-selectable *wprA* integration vector	This work
pAW010-4	P_{araE}::*mazF*, *araR*,Spc^R, Erm^R, *B. subtilis* counter-selectable *pssA* integration vector	This work
pAW011-4	P_{araE}::*mazF*, *araR*, Spc^R, Erm^R, *B. subtilis* counter-selectable *ugtP* integration vector	This work
Primer	**Sequence (5′–3′)[b]**	
P32	gctattgaccatggaaaaaagcaccgactcggt	
P122	cagattgaggatccatgtttaacttaccaaataaaatcacacta	
P123	ctcttatcctcctttgtacagattgcttagttagatgtttttaacgcttccca	
P124	gcaatctgtacaaaaggaggataagagaatgagtatttcttccatccttttatcac	
P125	agtaactaactagttataagatcggcgacaacag	
P126	ggtcatggatccgcaatatgcactgacgtctattctcc	
P127	tggtgcataggtcccgggataa	
P128	ggatctatgcaaccgtttttttcgg	
P129	cacagattgagctagcttctctccatggacgcgtgac	
P130	gctattgacctgcaggaattcatgtaaaagatgag	
P131	ccttccgaaaaaacggttgcatagatccgaaggcagcagttttttggcc	
P132	atcgatggatcactagaaaatttttttatcttatcacttgaaattgg	
P133	gataagataaaaaattttctagtgatccatcgatgaaggcagcagttttttggcc	
P134	tatgatgcatgc**attttcaatcattcggttaa**gttttagagctagaaatagcaagttaaa	
P135	cgcgtggcatgc**attttcaatcgttcggttaa**gttttagagctagaaatagcaagttaaa	
P136	gcacctgcatgc**atttttaatcattcggttaa**gttttagagctagaaatagcaagttaaa	
P137	tatgatgcatgc**ctgctctttgctttcttcag**gttttagagctagaaatagcaagttaaa	
P138	tatgatgcatgc**ctgctatttgctttcttcag**gttttagagctagaaatagcaagttaaa	
P139	tggaatgcatgc**tcgcggaatgcttcaagcat**gttttagagctagaaatagcaagttaaa	
P140	ctctacgacctgcaggatcaagtggatcacaggcgac	
P141	cagattgagctagccccatatcagaaacggcattcag	
P142	gtctactgggcgcgcccgacgtacagcatttgcggaat	
P143	cagacagaaccggtatgaataatccctataacccttccgattgt	
P144	ctcactgacctgcaggtttgcaaaaggcagcaacgagc	
P145	cagattgagctagccttccagttcggcgtctgtattcc	
P146	gtgactgaggcgcgccatgtggagcgcattgatgagc	
P147	cagattgaaccggttttgtatccatctccttcgatagctgt	
MCS[c]	gcaatatgcactgacgtctattctcctgcaggcattggatgcgcggcgcgcc **gaaaagaatgatggatcactagaaaatttttttaaaaaatctcttgacattgg** **aagggagatatgttattataagaattgcggaattgtgagcggataacaatt** **cccaattaaaggagg**aaactagttcatcacagttggccggcaactaaagt gcggcggccgccccggttgctgcgcgatcgcttgggaccataaaccggtt tatgacgttatcccgggacctatgcacca	

[a]: *amyE*, α-amylase; *lacA* (*ganA*): β-galactosidase; *mazF*, endoribonuclease (*Escherichia coli*); *thrC*, threonine synthase; *ugtP*, UDP-glucose diacylglycerol-transferase; *seHas*, hyaluronan synthase (*Streptococcus equisimilis*); *tuaD*, UDP-glucose-6 dehydrogenase; *xylR*, xylose operon repressor (*Bacillus megaterium*); *wprA*, cell wall-associated protease; d*cas9*, dead Cas9 (derived from *S. pyogenes*); *lacI*, lactose operon repressor (*E. coli*); *araR*, repressor of arabinose operons; *pssA*, phosphatidylserine synthase; Neo^R, neomycin resistance cassette; Erm^R, erythromycin resistance cassette; Spc^R, spectinomycin resistance cassette; Amp^R, ampicillin resistance cassette; [b], restriction sites used for cloning are underlined; inserted restriction sites are italicized; protospacer sequences are in bold font; substitutions in protospacers are in bold font and underlined; $P_{grac.max}$ and downstream ribosome binding site are in bold and italicized font; [c], synthesized as double-stranded DNA.

2.3 | HA production, purification, and analysis

HA production medium and seed culture preparation have been described previously (Westbrook et al., 2016), with some modifications. An overnight culture was used to inoculate flasks containing 25 ml prewarmed nonselect cultivation medium (20 g/L glucose) to an initial cell density of ~OD_{600} 0.1. Purification of HA and analysis of HA titer and MW were also performed as previously outlined (Westbrook et al., 2016).

2.4 | Fluorescence microscopy

B. subtilis strains were grown to mid-exponential growth phase prior to the addition of 10-*N*-nonyl-acridine orange (NAO; ThermoFisher Scientific; MA) in semi-defined medium with the following composition: $(NH_4)_2SO_4$, 0.83 g/L; K_2HPO_4, 5.82 g/L; KH_2PO_4, 2.5 g/L; trisodium citrate dihydrate, 417 mg/L; glucose, 4.17 g/L; $MgSO_4 \cdot 7H_2O$, 151 mg/L; yeast extract, 1.67 g/L; casamino acids, 208 mg/L; Arg, 7.5 g/L; His, 383 mg/L; Trp, 48 mg/L. *B. subtilis* strains were plated on non-select lysogeny broth (LB) agar containing 5 g/L NaCl, 5 g/L yeast extract, 10 g/L tryptone, and 15 g/L agar, and incubated overnight at 37°C. Pre-warmed medium (24 ml) was inoculated with cell patches from the overnight plate to OD_{600} 0.1–0.2, and cultured cells were grown to OD_{600} 0.3–0.5, at which time NAO was added to a final concentration of 1 μM. Cultures containing NAO were incubated in the dark at room temperature and 260 revolutions per min (rpm) for 25 min. The stained cells were then washed once in phosphate buffered saline (PBS; NaCl, 8 g/L; KCl, 0.2 g/L; Na_2HPO_4, 1.44 g/L; KH_2PO_4, 0.24 g/L) and resuspended in ProLong™ Live Antifade Reagent (ThermoFisher Scientific; MA) diluted 25-fold from the stock concentration. The stained cells were then mounted on object slides covered with agarose pads (1% wt/v in PBS). Fluorescence images were viewed using an Axio Imager D1 microscope and an AxioCam MRm camera (Carl Zeiss; Oberkochen, Germany). Green and red fluorescence from NAO was detected using standard filters, and exposure times were automatically set to less than 0.8 s. Captured images were processed using ImageJ (Schneider, Rasband, & Eliceiri, 2012).

3 | RESULTS

3.1 | Derivation of HA-producing strains of *B. subtilis*

Significant HA production can be achieved in strains of *B. subtilis* coexpressing only HAS and TuaD (Chien & Lee, 2007a; Jin et al., 2016; Widner et al., 2005), for which the expression is repressed in the presence of excess phosphate (Soldo, Lazarevic, Pagni, & Karamata, 1999). Accordingly, an HA-producing control strain was constructed by transforming *B. subtilis* 168 with NdeI-linearized pAW008 (Westbrook et al., 2016), a vector previously constructed for the integration of a P_{grac}::*seHas*:*tuaD* cassette at the *amyE* locus (Figure 1), yielding strain AW006 with a prominent mucoid phenotype characteristic of HA production in *B. subtilis* (Widner et al., 2005). However, for unknown reasons, AW006 formed a segregated population with the majority of cells being reverted to the wild-type phenotype upon strain revival. Such genetic instability was also an issue for AW007, an HA-producing 1A786 derivative constructed in the same manner as AW006. Consequently, 1A751 was selected as the production host due to its superior genetic stability based on the persistence of the mucoid phenotype of the HA-producing strain AW008, that is 1A751 transformed with NdeI-linearized pAW008. We then assessed HA production in shake flask cultures of AW008 as the control for comparison with other mutants. The cell density and HA titer reached OD_{600} 4.2 (Figure 2a) and 0.48 g/L (Figure 2b), respectively, after 10 hr, while the MW peaked at 1.95 MDa at 8 hr (Figure 2c). Decreasing MW with prolonged cultivation time has been reported for HA-producing strains of *B. subtilis* (Westbrook et al., 2016; Widner et al., 2005), and, therefore, the cultivations were terminated at 10 hr in light of declining MW. The HA titer compared favorably to a previous report of a similar HA-producing strain of *B. subtilis* (Chien & Lee, 2007a), as did the peak MW (Jin et al., 2016; Widner et al., 2005). In each case, *B. subtilis* 168 or its derivatives were used to coexpress SeHAS or SzHAS, and TuaD (Chien & Lee, 2007a; Jin et al., 2016; Widner et al., 2005). The improved culture performance of AW008 relative to similar HA-producing *B. subtilis* mutants may result, in part, from the promoter driving expression of SeHAS and TuaD. Specifically, the *grac* promoter (P_{grac}) was reported to be 30 times stronger than the commonly employed *xylA* promoter from *Bacillus megaterium* ($P_{xylA,\ Bm}$) (Phan et al., 2012), which was used to drive the expression of SzHAS in the aforementioned study (Jin et al., 2016). Medium composition may also be related to culture performance as minimal medium was used for HA production in some studies (Chien & Lee, 2007a; Widner et al., 2005), resulting in lower MWs compared to cultivation in complex medium based on our observations (data not published).

3.2 | Increased membrane CL content enhances HA production

Given the dependence of HAS activity on its orientation with CL in the membrane, we sought to assess the effects of increased membrane CL content on HA production. Accordingly, an HA-producing strain which produced more CL than the wild-type background was constructed by transforming AW008 with SacI-linearized pAW002-4, resulting in strain AW001-4, which constitutively expressed *pgsA* and *clsA* (regulated by promoter P_{grac}) from the *thrC* locus (Figure 1). Compared to the control strain AW008, the HA titer increased by 32% (0.63 g/L) for strain AW001-4 after 10 hr of cultivation (Figure 2b). Moreover, the peak MW was higher (2.06 MDa) and declined to a lesser extent between 8 and 10 hr of cultivation (Figure 2c), such that the MW of HA produced in cultures of AW001-4 after 10 hr was comparable to the peak MW in cultures of AW008. An 83% increase in the final cell density, that is OD_{600} 7.7 for AW001-4 versus 4.2 for AW008 (Figure 2a), was also observed, and the improved cell growth may partially explain the increased HA titer in cultures of AW001-4. We qualitatively assessed the CL levels in the membranes of our engineered strains using the CL-specific fluorescent dye NAO (Kawai et al., 2004; Nishibori et al., 2005).

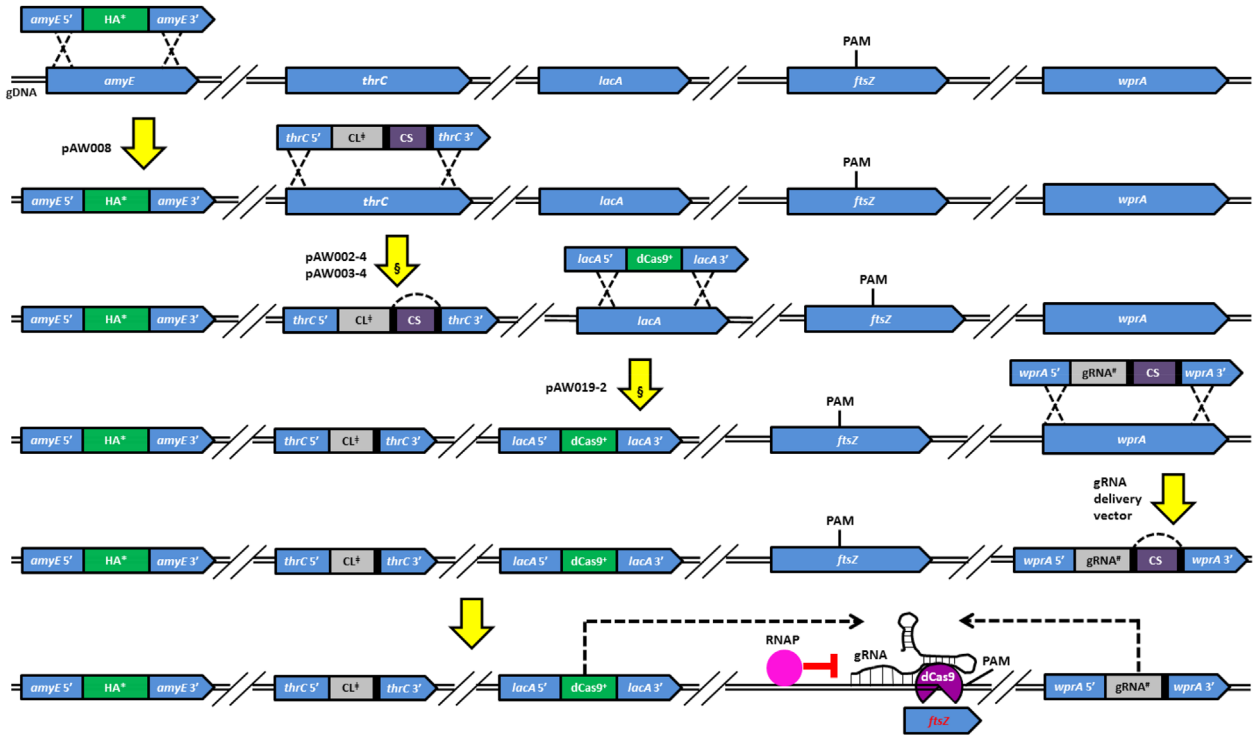

FIGURE 1 Genomic engineering strategies to enhance HA production in *B. subtilis*. The combined P_{grac}::*seHas*:*tuaD*-Neo^R (HA*) cassette was integrated into the *amyE* locus of 1A751 via transformation with pAW008, yielding strain AW008, which synthesizes HA. AW008 was then transformed with pAW002-4, resulting in integration of the P_{grac}::*pgsA*:*clsA* ($CL^‡$) cassette, and the combined P_{araE}::*mazF*-Spc^R (CS) cassette, at the *thrC* locus (the resulting mutant was spectinomycin resistant and arabinose sensitive). The CS cassette was subsequently auto-evicted via single-crossover recombination between the flanking direct repeats (black rectangles), yielding strain AW001-4 (spectinomycin sensitive and arabinose resistant), which overproduces CL. To generate strains in which expression of *ftsZ* was repressed, AW008 was first transformed with pAW019-2, resulting in integration of the combined $P_{xylA,\ Bm}$::*dcas9*-Erm^R ($dCas9^+$) cassette at the *lacA* locus, yielding strain AW002-4, which expresses xylose-inducible dCas9. AW002-4 was then transformed with either pAW002-4 or pAW003-4, resulting in integration of the P_{grac}::*pgsA*:*clsA* and $P_{grac.UPmod}$::*pgsA*:*clsA* ($CL^‡$) cassettes, respectively, and the CS cassette, at the *thrC* locus. The CS cassettes were subsequently auto-evicted, yielding respective strains AW003-4 and AW007-4, which both overproduce CL (AW003-4 produces more CL than AW007-4). AW003-4 was then transformed with pAW006-4, resulting in integration of the $P_{xylA.SphI+1}$::*ftsZ*-gRNA.P79NT(15C-U) ($gRNA^‡$) cassette, and the CS cassette, at the *wprA* locus. The CS cassette was subsequently auto-evicted, yielding strain AW004-4, which transcribes *ftsZ*-gRNA.P79NT(15C-U). AW007-4 was transformed with either pAW006-4, pAW007-4, pAW008-4, or pAW009-4, resulting in integration of the $P_{xylA.SphI+1}$::*ftsZ*-gRNA.P79NT(15C-U), $P_{xylA.SphI+1}$::*ftsZ*-gRNA.P244NT, $P_{xylA.SphI+1}$::*ftsZ*-gRNA.P244NT(15C-A), and $P_{xylA.SphI+1}$::*ftsZ*-gRNA.P533NT ($gRNA^‡$) cassettes, respectively, and the CS cassette, at the *wprA* locus. The CS cassettes were subsequently auto-evicted, yielding respective strains AW008-4, AW009-4, AW010-4, and AW011-4, which transcribe *ftsZ*-gRNA.P79NT(15C-U), *ftsZ*-gRNA.P244NT, *ftsZ*-gRNA.P244NT(15C-A), and *ftsZ*-gRNA.P533NT, respectively. The gRNAs direct dCas9 to the target (i.e., *ftsZ*) based on the presence of a PAM site and adjacent seed region complementary to the protospacer, and the dCas9-gRNA complex remains bound to the target, partially blocking transcription of *ftsZ* by RNA polymerase (RNAP). §The $dCas9^+$ cassette was chromosomally integrated prior to the $CL^‡$ cassette in strains in which *ftsZ* expression was repressed

Binding of NAO to CL results in the dimerization of NAO monomers, causing a shift in the emitted fluorescence peak of the monomer from green (at 525 nm) to red (at 640 nm) due to the metachromatic effect (Kawai et al., 2004). Red fluorescence was observed to co-localize with green fluorescence at the poles and septa of all strains analyzed, as exemplified in Figure 3a–c, in which green (Figure 3a) and red (Figure 3b) fluorescence emitted from NAO-stained AW008 co-localized in Figure 3c (i.e., an image generated by merging Figures 3a and 3b). The increased amount of CL in the membrane of AW001-4 was clearly visible (Figure 3d) based on the significantly higher fluorescence observed at the poles and septa of the cells, compared with AW008 (Figure 3c).

3.3 | Redistributing CL in the membrane further enhances HA production

The localization of CL at the poles and septal regions of the *B. subtilis* cell membrane during exponential growth presumably facilitates cell division through the formation of non-bilayer structures in the presence of divalent cations, such as Ca^{2+} or Mg^{2+} (Dowhan, 1997; Kawai et al., 2004). Given that SeHAS is a foreign protein to *B. subtilis* with no known homologue, it should not interact with other cellular machinery that may restrict its localization and distribution in the membrane. Also, as the intended function of Class I HAS in streptococci is to encapsulate the entire cell to prevent recognition

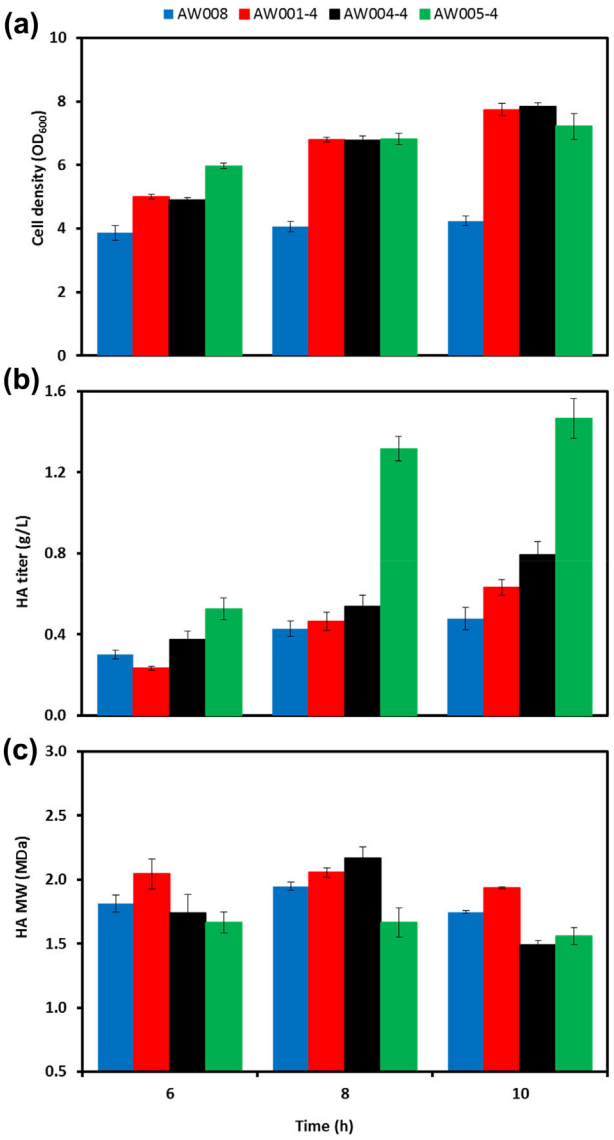

FIGURE 2 Time profiles of (a) cell density, (b) HA titer, and (c) HA MW in cultures of AW008, AW001-4, AW004-4, and AW005-4. SD of experiments performed in triplicate are shown in Panels a and b, and SD of duplicate samples are shown in Panel c

by the host immune response (Tlapak-Simmons, Baron, & Weigel, 2004), SeHAS may be distributed throughout the membrane of *B. subtilis*. We hypothesized that a narrow distribution of CL in the *B. subtilis* cell membrane could reduce its interaction with SeHAS, such that altering the distribution of CL may increase its availability to SeHAS, thereby enhancing the functional expression of the enzyme. Accordingly, we sought to tune the expression of *ftsZ* to redistribute CL along the lateral membrane in AW001-4. Recently, we developed a CRISPR-Cas9 toolkit enabling both genome editing and transcriptional interference in *B. subtilis* (Westbrook et al., 2016). To apply CRISPRi for the purpose of modulating *ftsZ* expression, AW008 was transformed with BseYI-linearized pAW019-2 (Westbrook et al., 2016), yielding strain AW002-4 in which xylose-inducible dCas9 was expressed from the *lacA* locus (Figure 1). AW002-4 was subsequently transformed with SacI-linearized pAW002-4, generating strain AW003-4 which is a CL-overproducing strain suitable for evaluation of various gRNAs targeting *ftsZ*. Six *ftsZ*-targeting gRNAs were designed to cover the range of relative repression efficiency by manipulating gRNA design parameters previously described (Larson et al., 2013; Qi et al., 2013). Mismatches introduced in base pairs (bp) 8–12 of the protospacer (relative to the 3′-end) cause a dramatic reduction in repression efficiency, while mismatches in bp 13–20 have a reduced effect on repression efficiency (Note that the first 7 bp should not be altered.) (Larson et al., 2013; Qi et al., 2013). Moreover, repression levels are roughly inversely proportional to the distance between the selected PAM site and the start codon of the target open reading frame (ORF) (Larson et al., 2013; Qi et al., 2013). We chose PAM sites P79NT, P244NT, and P533NT, which correspond to relative distances of 0.06, 0.21, and 0.46, respectively, from the start codon (Note that the first bp of the start codon and last bp of the stop codon correspond to relative distances of 0 and 1, respectively). Based on proximity to the start codon alone, the relative repression efficiency afforded by targeting PAM sites P79NT, P244NT, and P533NT were estimated to be 1, 0.8, and 0.4, respectively (Qi et al., 2013). Mismatches were introduced in the protospacer at position 10 and 15 to further reduce the relative repression efficiency by ~75% and ~30%, respectively. We assumed that the effects of PAM site selection and mismatches introduced in the protospacer were multiplicative when estimating the overall relative repression efficiency. For example, the relative repression efficiency of *ftsZ* expression resulting from transcription of *ftsZ*-gRNA.P244NT(15C-A) was estimated to be $0.8 \times 0.7 = 0.56$. Table 2 summarizes various *ftsZ*-targeting gRNAs with their corresponding protospacer sequence and estimated relative repression efficiency.

Of the six gRNA delivery vectors constructed, only pAW006-4, containing *ftsZ*-gRNA.P79NT(15C-U), could be stably transformed into AW003-4 as the resulting strain AW004-4 maintained the mucoid phenotype upon revival from a glycerol stock. Interestingly, AW004-4 produced 65% and 25% more HA than AW008 and AW001-4, respectively, after 10 hr cultivation (0.79 g/L; Figure 2b), while the peak MW of 2.17 MDa obtained at 8 hr was a moderate improvement relative to either strain (Figure 2c). However, the MW decreased substantially to 1.49 MDa after 10 hr, resulting in a lower overall MW than AW008 or AW001-4. Note that the growth profile of AW004-4 was nearly identical to that of AW001-4, with the final cell density reaching OD_{600} 7.8 (Figure 2a). Fluorescence microscopy revealed a moderate reduction in the fluorescence intensity of CL domains in the membrane of AW004-4 (Figure 3e), compared to AW001-4 (Figure 3d), indicating that partial redistribution of CL along the lateral membrane of AW004-4 had occurred, presumably due to reduced *ftsZ* expression. Furthermore, a moderate degree of filamentation was observed for AW004-4 (Figure 3e).

We then examined the effect of dCas9 expression on HA production using cultures of AW004-4 induced with xylose under different concentrations. No significant change in the HA titer, MW or cell growth was observed except at the highest xylose concentration of 1% wt/v, which resulted in decreases to the titer

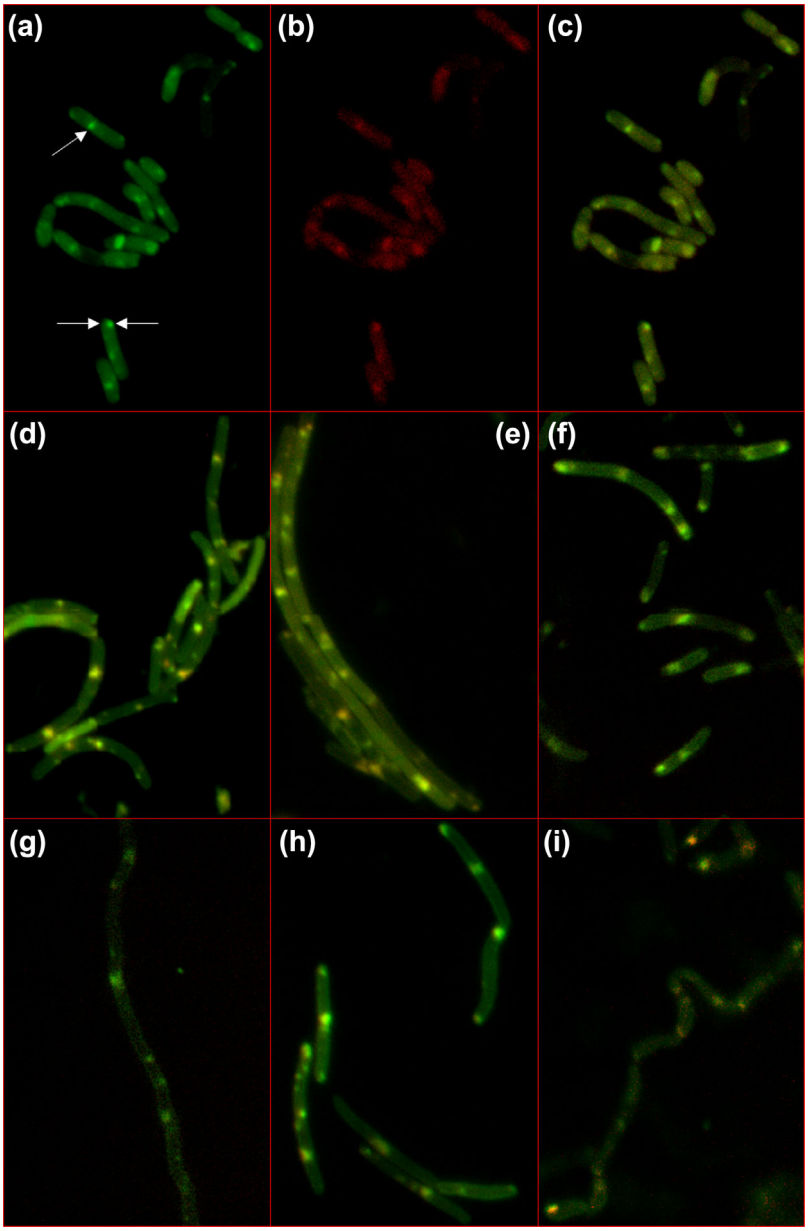

FIGURE 3 Representative images of strains of *B. subtilis* stained with NAO obtained with fluorescence microscopy. Panels a and b display green and red fluorescence emitted by AW008, respectively, and Panels c (AW008), d (AW001-4), e (AW004-4), f (AW007-4), g (AW009-4), h (AW010-4), and i (AW011-4) are merged images of green and red fluorescence emitted by respective strains. The single arrow indicates localization of CL at the septal region of the cell membrane, and the double arrows indicate localization of CL at the pole in Panel a. NAO was added to cultures during mid-exponential growth phase to a final concentration of 1 μM, followed by incubation in the dark at room temperature and 260 rpm for 25 min. Stained cells were then washed once in PBS and resuspended in ProLong™ Live Antifade Reagent diluted 25-fold from the stock concentration, prior to mounting on object slides as described in M&M

and cell density after 10 hr (Figure 4). These observations may be explained by a visible increase in filamentation in cultures induced with 1% wt/v xylose, resulting in large aggregate formation in the flasks, skewing cell density measurements, and potentially disrupting the extracellular release of HA. The results suggest that tailoring transcriptional repression via CRISPRi by adjusting dCas9 expression may be ineffective (Larson et al., 2013), while manipulating the protospacer sequence and PAM site selection may provide more control over repression efficiency.

3.4 | Targeting *ftsZ* for CL redistribution is sensitive to CL or ClsA levels in the membrane

To separate the effects of reduced *ftsZ* expression and increased membrane CL content on HA production as well as to determine if the poor transformability of gRNA delivery vectors bearing *ftsZ*-targeting gRNAs was related to elevated CL levels in AW003-4, AW002-4 was transformed with pAW006-4 and pAW007-4, which could not be transformed into AW003-4, yielding genetically stable

TABLE 2 *ftsZ*-targeting gRNAs and their respective protospacer sequence and estimated relative repression efficiency

gRNA	Protospacer sequence[a]	Relative repression efficiency
ftsZ-gRNA.P79NT	ATTTTCAATCATTCGGTTAA	1
ftsZ-gRNA. P79NT(10A-G)	ATTTTCAATCGTTCGGTTAA	0.25
ftsZ-gRNA. P79NT(15C-U)	ATTTTTAATCATTCGGTTAA	0.7
ftsZ-gRNA. P244NT	CTGCTCTTTGCTTTCTTCAG	0.8
ftsZ-gRNA. P244NT(15C-A)	CTGCTATTTGCTTTCTTCAG	0.56
ftsZ-gRNA. P533NT	TCGCGGAATGCTTCAAGCAT	0.4

[a]Mismatches are underlined.

strains AW005-4 and AW006-4, respectively. The observation that AW002-4, but not AW003-4, could be transformed with pAW007-4 suggests that the impact of reduced *ftsZ* expression on cell physiology was related with the level of CL (or ClsA) in the membrane. Accordingly, AW002-4 was transformed with SacI-linearized pAW003-4, generating strain AW007-4 containing a $P_{grac.UPmod}$::*pgsA*:*clsA* cassette at the *thrC* locus (Figure 1). Promoter $P_{grac.UPmod}$ is a weaker derivative of promoter P_{grac} with the relative promoter strength of ~0.5 (Phan et al., 2012), and fluorescence microscopy confirmed the reduced CL levels in the membrane of AW007-4 (Figure 3f), compared to AW001-4 (Figure 3d). AW007-4 was subsequently transformed with pAW006-4, pAW007-4, pAW008-4, and pAW009-4, yielding genetically stable strains AW008-4, AW009-4, AW010-4, and AW011-4, respectively, with the mucoid phenotype upon revival from glycerol stocks (Note that pAW004-4 and pAW005-4 could not be transformed into AW007-4.). The enhanced transformability of AW007-4 associated with gRNA delivery vectors containing *ftsZ*-targeting gRNAs confirmed that the sensitivity of strains of *B. subtilis* to reduced *ftsZ* expression was dependent on membrane CL (or ClsA) levels. Our results are consistent with the previous observation that the distribution of ClsA in the membrane is dependent on FtsZ or some other component(s) of the cell division machinery (Nishibori et al., 2005).

Upon transformation of AW003-4 and AW007-4 with pAW006-4, distinct changes in morphology were observed for the resulting strains AW004-4 and AW008-4. AW004-4 formed small colonies surrounded by a clear HA capsule for which the thickness could be visually distinguished from the edge of the colony. As expected, the colonies had a stringy texture associated with cell filamentation resulting from reduced *ftsZ* expression (Nishibori et al., 2005). On the other hand, AW008-4, with a lower CL level than AW004-4, formed large colonies and more resembled the parent strain, suggesting that the effects of repression of *ftsZ* expression on cell physiology are related to CL levels in the membrane. In addition, AW010-4 formed relatively large colonies (though not as large as

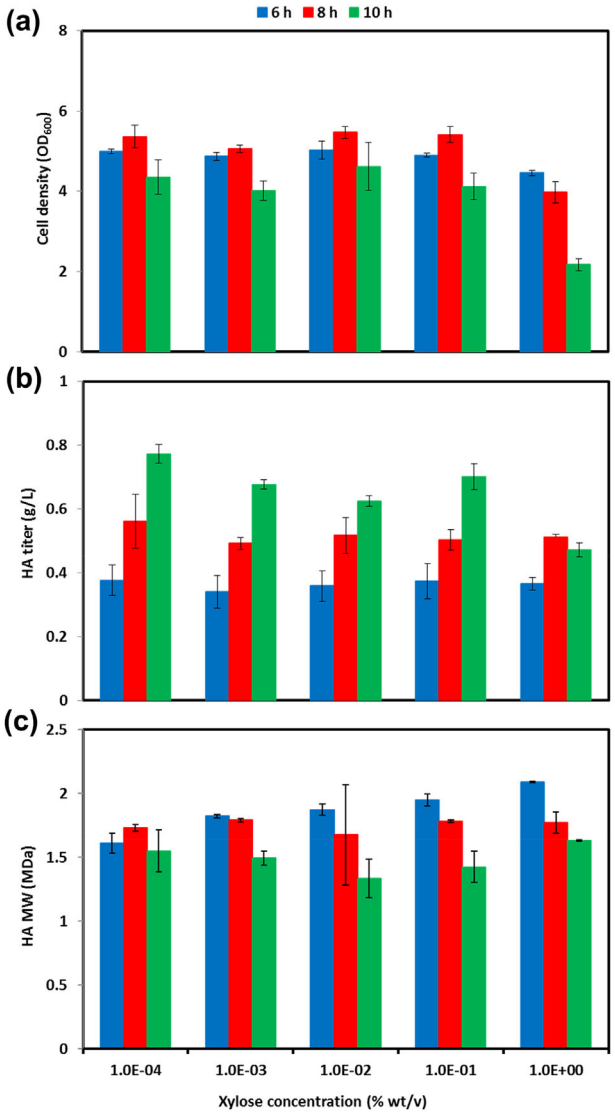

FIGURE 4 Time profiles of (a) cell density, (b) HA titer, and (c) HA MW in cultures of AW004-4 induced with xylose 2 hr after inoculation. SD of experiments performed in duplicate are shown

AW004-4) with a less stringy texture (but more stringy than AW008-4) compared to AW004-4. AW009-4 and AW011-4 formed very small translucent colonies for which the HA capsule could not be distinguished from the colony, as was the case for AW004-4, and the colonies had a more stringy texture than AW004-4. Fluorescence microscopy revealed a significant degree of CL redistribution along the lateral membrane of AW009-4 (Figure 3g) and AW011-4 (Figure 3i), while the membrane CL distribution in AW010-4 (Figure 3h) was less drastically altered. Similarly, extensive filamentation of AW009-4 (Figure 3g) and AW011-4 (Figure 3i) occurred, while AW010-4 (Figure 3h) retained a morphology similar to that of AW007-4 (Figure 3f). Based on the results of fluorescence microscopy, cell morphology, and the transformation efficiencies associated with various gRNA delivery vectors, the highest relative repression efficiency of *ftsZ* expression resulted from transcription of *ftsZ*-gRNA.P244NT, followed by *ftsZ*-gRNA.P533NT, *ftsZ*-gRNA.

P244NT(15C-A), and *ftsZ*-gRNA.P79NT(15C-U), in the order of declining repression efficiency.

Mutants transcribing *ftsZ*-targeting gRNAs derived from AW002-4 (i.e., AW005-4) and AW007-4 (i.e., AW008-4, AW009-4, AW010-4, and AW011-4) were further evaluated for HA production in shake flask cultures. AW005-4 produced 204% and 85% more HA than AW008 and AW004-4, respectively, with the titer reaching 1.46 g/L after 10 hr (Figure 2b). While the peak MW was only 1.67 MDa after 8 hr in cultures of AW005-4 (Figure 2c), the MW did not decline substantially afterwards, and was slightly higher than the MW of HA produced in cultures of AW004-4 after 10 hr (Figure 2c). The culture performance of AW004-4 (Figure 2a–c) and AW008-4 (Figure 5a–c) was similar, with the MW of HA and cell density of AW008-4 being slightly lower. Notably, AW011-4 produced 1.25 g/L of HA after only 8 hr (Figure 5b), while the MW reached 2.10 MDa and declined slightly by 10 hr (Figure 5c).

4 | DISCUSSION

HA synthesis is an intricate process performed by Class I or II HAS, with the former being a relatively small integral membrane protein which requires precisely coordinated lipid molecules to autonomously polymerize and extrude the growing HA chain. Here, we have shown that engineering of the cell membrane can enhance heterologous HA production in *B. subtilis* expressing SeHAS. Given that the activity of streptococcal Class I HAS is restored upon reconstitution of the purified enzyme with CL in vitro (Tlapak-Simmons et al., 1999; Triscott & van de Rijn, 1986), it is plausible that the presence and distribution of CL in the cell membrane can critically affect HA synthesis and even secretion. However, the results of a prior study in *S. pyogenes* (Rosch, Hsu, & Caparon, 2007) and ours suggest that the lipid dependence of streptococcal Class I HAS in vitro may be less flexible than its lipid dependence in vivo.

Microbial cultivation has become the dominant method of industrial HA production in recent years (Liu et al., 2011). Group C streptococci (e.g., *S. zooepidemicus*) are the most commonly employed production hosts, due to their capability to produce HA of MWs up to 5.9 MDa, with titers reaching 7 g/L (Im, Song, Kang, & Kang, 2009; Kim et al., 1996). However, the production of exotoxins, poor growth characteristics and extensive nutritional requirements, and lack of genetic tractability (Vázquez et al., 2010; Widner et al., 2005) prompted exploration of alternate microbial HA production platforms. *Lactococcus lactis* is a promising candidate for industrial HA production as it has been granted GRAS status, tools are available for its genetic manipulation, and it has produced HA titers of up to 1.8 g/L in batch cultivations (Prasad, Jayaraman, & Ramachandran, 2010). While the nutritional requirements of *L. lactis* are simple, its slow growth rate can potentially result in higher biomanufacturing costs. High-level heterologous HA production has also been achieved in *Streptomyces albulus*, which can generate significant quantities of ATP required for the natural production of ε-poly-L-lysine (Yoshimura et al., 2015). As a result, an HA titer of 6.2 g/L was obtained in a fed-batch cultivation,

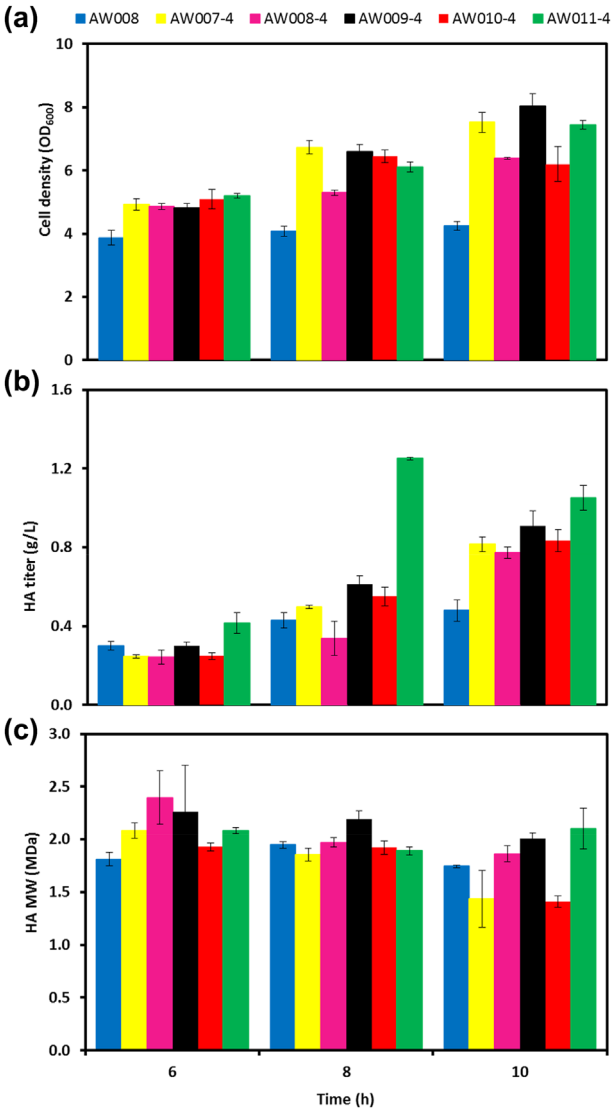

FIGURE 5 Time profiles of (a) cell density, (b) HA titer, and (c) HA MW in cultures of AW008, AW007-4, AW008-4, and AW009-4, AW010-4, and AW011-4. SD of experiments performed in triplicate are shown in Panels a and b, and SD of duplicate samples are shown in Panel c

which is comparable to that obtained in streptococcal cultivations. However, the application of *S. albulus* to biomanufacturing may be limited by slow growth, relatively difficult genetic manipulation, problems expressing HAS, and lack of GRAS status (Yoshimura et al., 2015). Heterologous HA production has also been achieved with some success in the yeast *Pichia pastoris* (Jeong, Shim, & Kim, 2014). While highly amenable to genetic manipulation and commonly employed for recombinant protein expression (Ahmad, Hirz, Pichler, & Schwab, 2014), *P. pastoris* grows slowly and its HA production capacity is poor compared to bacteria (up to 1.7 g/L HA produced after 48 hr fed-batch cultivation) (Jeong et al., 2014). *E. coli* has also been used as a host for heterologous HA production, generating titers of up to 3.8 g/L with GlcNAc supplementation (Mao et al., 2009). While *E. coli* is the preferred industrial bacterium for biomanufacturing for well-known reasons, its use is still hampered by endotoxin contamination of its

products (Mamat et al., 2015). Of all the non-native hosts used for heterologous HA production to date, *B. subtilis* may show the most promise. We have obtained a HA titer of 3.5 g/L in a 10 hr batch cultivation of AW008 (data not shown), and fed-batch cultivation has led to titers exceeding 7 g/L (Widner et al., 2005). High production capacity coupled with easy genetic manipulation, excellent growth on simple media, and GRAS status, make *B. subtilis* an ideal choice for industrial HA production. However, *B. subtilis*, like all other heterologous producers of HA investigated to date, produce lower MW HA than group C streptococci. Accordingly, improving the MW of heterologously produced HA is currently the major challenge to be addressed with advanced strain engineering strategies.

The significant increase in the amount of CL in AW001-4 (Figure 3d), compared with AW008 (Figure 3c), was associated with the increased levels of *pgsA* and *clsA*. The relative membrane CL levels between AW001-4 (Figure 3d) and AW007-4 (Figure 3f) appeared to be less significant given that the strength of promoter P_{grac} is only twice that of promoter $P_{grac.UPmod}$ (Phan et al., 2012). On the other hand, the enhanced transformability of gRNA delivery vectors containing *ftsZ*-targeting gRNAs in AW007-4, compared to AW003-4, suggests that membrane CL levels may be significantly different between the two strains. Comparison of the culture performance of both AW001-4 and AW007-4 to AW008 shows that moderation of the membrane CL content (based on the use of different promoters driving the expression of *pgsA* and *clsA*) may provide similar improvements to cell density, while resulting in a higher titer and lower MW of HA for AW007-4. This suggests that a higher amount of CL in the membrane may have increased the functional expression of SeHAS, although the increased CL synthesis may have simultaneously diminished the carbon flux available for HA production. The addition of CL to purified SeHAS or SpHAS resulted in the highest enzyme activity in vitro, compared to the addition of other lipids (Tlapak-Simmons et al., 1999; Triscott & van de Rijn, 1986), and exogenous CL was shown to enhance the activity of both enzymes in the membrane fractions of *E. coli* cells, suggesting that the ratio of CL to HAS was not high enough to maximize the activity of heterologously expressed HAS (Tlapak-Simmons et al., 1998). It was revealed that controlling chain length and polymerizing activity are independent functions of SeHAS that are not coupled to one another (Weigel & Baggenstoss, 2012), although CL may play dual roles in chain elongation. CL may assist HAS in the formation of pores in the cell membrane through which the growing HA chain is translocated (Tlapak-Simmons et al., 1998), and its interaction with HA may contribute to the net force required to retain the chain as it is extended . Accordingly, increased CL availability in the cell membrane of HA-producing *B. subtilis* could enable more of the total expressed enzyme per cell to achieve higher activity (i.e., higher polymerization rate) and improved functionality with regard to the retention and translocation of the growing HA chain, resulting in the improved functional expression of SeHAS. This may partially explain the improved culture performance of AW001-4, compared to AW008, although the lower specific HA titer (Figure 6) indicates that overproduction of CL competed with HA synthesis for glucose. This point is supported by the nearly identical specific HA titers in cultures

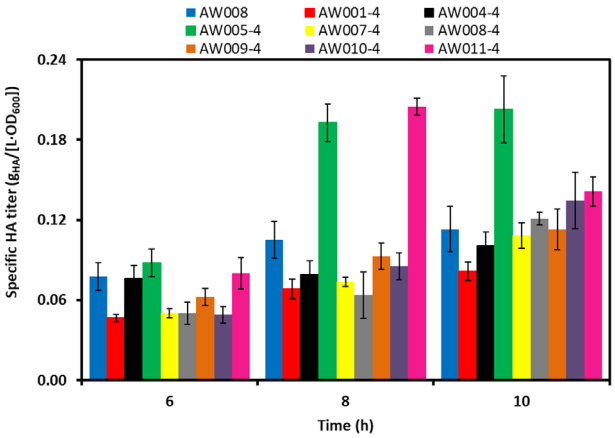

FIGURE 6 Time profiles of the specific HA titer in cultures of AW008, AW001-4, AW004-4, AW005-4, AW007-4, AW008-4, and AW009-4, AW010-4, and AW011-4. SD of experiments performed in triplicate are shown

of AW007-4 and AW008 (Figure 6), and the similar final cell densities observed in cultures of AW001-4 (Figure 2a) and AW007-4 (Figure 5a), such that further increasing CL production in AW001-4, compared to AW007-4, reduced the HA titer without affecting biomass accumulation. Accordingly, optimizing the expression of *pgsA* and *clsA* may be necessary to balance the MW and HA titer in HA-producing strains of *B. subtilis*. Deletion of *cls*, encoding the sole CL synthase, in *Streptococcus mutans* significantly increased the doubling time and reduced the final cell density in acidic medium, relative to the parent strain, while growth characteristics were identical between both strains in neutral medium (MacGilvray et al., 2012). CL has also been implicated in the adaptive response of *B. subtilis* to conditions of high salinity (Lopez, Alice, Heras, Rivas, & Sanchez-Rivas, 2006). The poor oxygen mass transfer and lack of pH control in shake flask cultures can result in their acidification as the culture progresses, such that the initial pH in our cultivations (i.e., pH 7) would have declined by the end of the cultivation. The enhanced cell growth in cultures of AW001-4, compared to AW008, suggests that increasing the amount of CL in the *B. subtilis* membrane may improve the acid-adaptive response. However, we observed that the exponential growth rates of both AW008 and AW001-4 declined by ~30%, while the respective final cell densities increased and decreased by 10% and 24% in medium titrated to pH 6 (data not shown). Furthermore, AW001-4 did not grow, while the logarithmic growth rate and final cell density of AW008 did not change (although the length of the lag phase increased by 60%) as the initial pH of the medium was further reduced to 5.7. Accordingly, the improved growth of AW001-4, compared to AW008, does not appear to be related to an improved acid-adaptive response. Further investigation is required to elucidate the mechanism(s) through which cell physiology was improved upon increasing the membrane CL level. As HA is a growth-associated product (Huang, Chen, & Chen, 2006), the increased HA titers in cultures of CL-overproducing strains can be explained, in part, by their improved growth, which is evident from the similar specific HA titers observed in cultures of AW007-4 and AW008 (Figure 6).

While higher cell densities were achieved in cultivation medium with strains in which expression of *ftsZ* was repressed, relative to AW008, the opposite behavior was observed for cultures with LB medium, that is the final cell density of overnight LB cultures of AW008 were higher in each case (data not shown). The improved growth of these strains in cultivation medium may have resulted from the presence of divalent metals, which have been shown to enhance self-assembly of high MW FtsZ oligomers in vitro (Monterroso et al., 2012). Moreover, Z-ring formation is coupled to pyruvate levels via the E1α subunit of pyruvate dehydrogenase (Monahan, Hajduk, Blaber, Charles, & Harry, 2014), such that cultivation medium containing glucose may enhance FtsZ polymerization relative to LB which lacks a preferred carbon source. The relatively small amount and narrow spatial distribution of CL in the cell membrane of *B. subtilis* may result in CL levels which are not sufficient to maximize the functional expression of SeHAS, which was observed in *E. coli* heterologously expressing streptococcal Class I HAS (Tlapak-Simmons et al., 1998). Note that CL localizes at the poles and septal regions of the cell membrane in both *E. coli* and *B. subtilis* (Kawai et al., 2004; Mileykovskaya & Dowhan, 2000). Thus, the functional expression of SeHAS may be improved by redistributing CL along the lateral membrane, which may partially explain the increased MW and HA titers observed in cultures of certain strains in which expression of *ftsZ* is repressed. The redistribution of natural CL without carbon being siphoned away from HA production to accommodate CL overproduction, may partially explain the significantly improved HA titer obtained in cultures of AW005-4, relative to all other strains. However, the reduced peak MW of HA produced in cultures of AW005-4, compared to AW008, was unexpected, given that AW004-4 and strains derived from AW007-4 in which *ftsZ* expression was repressed, produced HA of an equivalent or higher peak MW compared to their respective parent strains. Moreover, the significantly increased specific HA titer in cultures of AW005-4, compared to AW008 (Figure 6), may indicate that more glucose was available for HA synthesis due to the reduced expression of FtsZ. Taken together, the increased specific HA titer and reduction in MW in cultures of AW005-4, compared to AW008, suggest that improved carbon flux through the HA biosynthetic pathway, rather than the enhanced functional expression of SeHAS, had a greater impact on the culture performance of AW005-4. In general, an increase in the specific HA titer was observed in cultures of strains in which expression of *ftsZ* was repressed, compared to their respective parent strains, which could be partially attributed to increased carbon availability for HA synthesis due to reduced FtsZ expression, and/or reduced biomass accumulation in the case of AW008-4 and AW010-4. The improved HA titer in cultures of AW011-4, compared to AW008-4 and AW010-4 (Figure 5b), suggests that the repression of *ftsZ* expression was conducive to HA production in *B. subtilis*. On the other hand, a further increase in repression efficiency may reduce the HA titer, as observed in cultures of AW009-4 (Figure 5b), without significantly affecting the MW. The results suggest that a delicate balance between the CL level and distribution in the cell membrane of *B. subtilis* appears to be critical for optimization of culture performance for heterologous HA production.

The improvements to the MW of HA produced by most engineered *B. subtilis* strains possessing CL-enriched membranes in this study was modest. This is not entirely surprising given that a *cls* (encoding CL synthase) deficient *S. pyogenes* mutant retained the full ability to produce the HA capsule, relative to the parent strain which constitutively produced HA due to a mutation of the transcriptional regulator CovR (Rosch et al., 2007). Moreover, the titer and MW of HA produced by strains of *B. subtilis* expressing only SeHAS and TuaD were comparable to those based on streptococcal cultivations (Widner et al., 2005), in spite of the relatively small amount of CL naturally present in the *B. subtilis* membrane. Similarly, heterologous HA production was achieved in a variety of bacterial hosts expressing Class I HAS from group C streptococci without alterations to the host membrane (Chien & Lee, 2007b; Yoshimura et al., 2015; Yu & Stephanopoulos, 2008). Accordingly, it appears that alternate lipids may suffice to assist bacterial Class I HAS in HA synthesis. The *B. subtilis* membrane is composed mainly of PG (the only essential lipid) and phosphatidylethanolamine (PE), in addition to a large amount of neutral glycolipids (GL) (Salzberg & Helmann, 2008). The dependence of SeHAS activity on PG could not be assessed in vivo in *B. subtilis* as *pgsA* mutants are not viable (Kobayashi et al., 2003). However, PG was observed to have no stimulatory effect on the activity of purified SeHAS in vitro (Tlapak-Simmons et al., 1999). To determine if either of the other major lipids present in the *B. subtilis* membrane, that is PE and GL, were critical in maintaining the activity of SeHAS, we respectively mutated *pssA* (encoding PssA, an enzyme for synthesizing phosphatidylserine, which is subsequently converted to PE) and *ugtP* (encoding UDP-glucose diacylglyceroltransferase; UgtP, an enzyme involved in the conversion of PA to GL, Salzberg & Helmann, 2008) in AW008 via transformation of respective plasmids pAW010-4 and pAW011-4, generating respective mutant strains AW012-4 and AW013-4. The HA titers obtained in cultures of AW012-4 and AW013-4 were not significantly different from that obtained in cultures of AW008 (data not shown). The fact that PE deficiency did not significantly alter HA production in *B. subtilis* was not surprising, given that PE marginally enhanced the activity of purified SeHAS in vitro (Tlapak-Simmons et al., 1999), and that, like CL, PE localizes at the septal regions of the membrane in *B. subtilis* (Nishibori et al., 2005). On the other hand, UgtP is involved in the synthesis of diglucosyldiacylglycerol, the membrane anchor for lipoteichoic acids (Percy & Gründling, 2014; Salzberg & Helmann, 2008), and in the coupling of nutrient availability to cell division by potentially inhibiting Z ring formation in nutrient rich conditions (Shiomi & Margolin, 2007), such that its mutation results in pronounced growth defects (Percy & Gründling, 2014; Salzberg & Helmann, 2008). Regardless of the physiological defects arising from UgtP deficiency, AW013-4 reached a similar cell density to AW008 with a comparable HA titer, suggesting that SeHAS might not preferentially coordinate with GL. Based on our results and the previous observation of HA synthesis in *cls*-deficient *S. pyogenes* whose membrane is composed primarily of CL, PG, and GL (Rosch et al., 2007), PG may satisfy the lipid requirements of streptococcal Class I HAS in vivo. Our results also suggest that HA synthesis in *B. subtilis* is a robust process potentially insensitive to major physiological perturbations in the host.

The estimated relative repression efficiencies of *ftsZ*-targeting gRNAs did not agree well with our experimental observations, particularly in terms of transformability, morphology, and microscopy

analysis. For example, *ftsZ*-gRNA.P79NT(10A-G) was expected to provide the lowest degree of repression of *ftsZ* expression, but it appeared to show a high level of repression relative to four of the other five gRNAs tested, and the nature of the substitution may be associated with the observed high level of repression. On the other hand, *ftsZ*-gRNA.P79NT(15C-U) resulted in the lowest level of repression of *ftsZ* expression while it was anticipated to provide a high repression level of 0.7. A recent investigation of the kinetics of dCas9 binding to off-target sequences indicated that the apparent association rates for targets in which A-G mismatches had been introduced outside of the seed region (Note that the seed region includes the first seven bp adjacent to the PAM site.) were typically high (Boyle et al., 2017). Substitution of an A with a G residue could potentially result in a G-T wobble base pair (in which hydrogen bonds link N1 of G with O2 of T and O6 of G with N3 of T) which can be accommodated in biologically active double-stranded DNA (Kennard, 1985). A poly(T) signal and/or more stable hairpin structure in the protospacer of *ftsZ*-gRNA.P79NT-(15C-U) may have led to low repression of *ftsZ* expression in AW004-4 and AW008-4. The protospacer of *ftsZ*-gRNA.P79NT is expected to form a minimally stable hairpin structure ($\Delta G = -2.46$ kcal/mole), although substitution of the C with a U residue at position 15 for *ftsZ*-gRNA. P79NT(15C-U) may result in the formation of a more stable hairpin structure ($\Delta G = -4.07$ kcal/mole). While the poly(T) signal is a distinguishing characteristic of rho-independent terminators in bacteria, its presence alone is typically not sufficient to achieve efficient transcription termination (Abe & Aiba, 1996; Nudler, Kashlev, Nikiforov, & Goldfarb, 1995), as is the case in eukaryotes (Pagano et al., 2007). Accordingly, it is likely that hairpin formation in the protospacer may disrupt base pairing between the gRNA and the DNA target. Evidently, tuning repression efficiency by introducing mismatches in the protospacer of gRNAs when applying CRISPRi is a complicated and trial-and-error process, given the availability of a meticulous gRNA design protocol. On the other hand, the selection of PAM sites based on their proximity to the beginning of the target ORF may provide more control over relative repression efficiency without enabling precise adjustment to target gene expression.

ACKNOWLEDGMENTS

We thank Sarah Schoor and Simon D.X. Chuong for their assistance in performing fluorescence microscopy.

ORCID

C. Perry Chou http://orcid.org/0000-0002-7254-8118

REFERENCES

Abe, H., & Aiba, H. (1996). Differential contributions of two elements of rho-independent terminator to transcription termination and mRNA stabilization. *Biochimie*, *78*(11), 1035–1042.

Ahmad, M., Hirz, M., Pichler, H., & Schwab, H. (2014). Protein expression in *Pichia pastoris*: Recent achievements and perspectives for heterologous protein production. *Applied Microbiology and Biotechnology*, *98*(12), 5301–5317.

Boyle, E. A., Andreasson, J. O., Chircus, L. M., Sternberg, S. H., Wu, M. J., Guegler, C. K., . . . Greenleaf, W. J. (2017). High-throughput biochemical profiling reveals sequence determinants of dCas9 off-target binding and unbinding. *Proceedings of the National Academy of Sciences*, *114*(21), 5461–5466.

Burkholder, P. R., & Giles, N. H., Jr. (1947). Induced biochemical mutations in *Bacillus subtilis*. *American Journal of Botany*, *34*(6), 345–348.

Cao, H., Heel, A. J., Ahmed, H., Mols, M., & Kuipers, O. P. (2017). Cell surface engineering of *Bacillus subtilis* improves production yields of heterologously expressed α-amylases. *Microbial Cell Factories*, *16*(1), 56.

Chen, R. (2007). Permeability issues in whole-cell bioprocesses and cellular membrane engineering. *Applied Microbiology and Biotechnology*, *74*(4), 730–738.

Chien, L.-J., & Lee, C.-K. (2007a). Enhanced hyaluronic acid production in *Bacillus subtilis* by coexpressing bacterial hemoglobin. *Biotechnology Progress*, *23*(5), 1017–1022.

Chien, L.-J., & Lee, C.-K. (2007b). Hyaluronic acid production by recombinant *Lactococcus lactis*. *Applied Microbiology and Biotechnology*, *77*(2), 339–346.

Chong, B., Blank, L., McLaughlin, R., & Nielsen, L. (2005). Microbial hyaluronic acid production. *Applied Microbiology and Biotechnology*, *66*(4), 341–351.

Chou, C. P. (2007). Engineering cell physiology to enhance recombinant protein production in *Escherichia coli*. *Applied Microbiology and Biotechnology*, *76*(3), 521–532.

DeAngelis, P. L., Jing, W., Drake, R. R., & Achyuthan, A. M. (1998). Identification and molecular cloning of a unique hyaluronan synthase from *Pasteurella multocida*. *Journal of Biological Chemistry*, *273*(14), 8454–8458.

DeAngelis, P. L., Papaconstantinou, J., & Weigel, P. H. (1993). Molecular cloning, identification, and sequence of the hyaluronan synthase gene from group A *Streptococcus pyogenes*. *Journal of Biological Chemistry*, *268*(26), 19181–19184.

Dowhan, W. (1997). Molecular basis for membrane phospholipid diversity: Why are there so many lipids? *Annual Review of Biochemistry*, *66*(1), 199–232.

Goa, K., & Benfield, P. (1994). Hyaluronic acid. *Drugs*, *47*(3), 536–566.

Härtl, B., Wehrl, W., Wiegert, T., Homuth, G., & Schumann, W. (2001). Development of a new integration site within the *Bacillus subtilis* chromosome and construction of compatible expression cassettes. *Journal of Bacteriology*, *183*(8), 2696–2699.

Huang, W.-C., Chen, S.-J., & Chen, T.-L. (2006). The role of dissolved oxygen and function of agitation in hyaluronic acid fermentation. *Biochemical Engineering Journal*, *32*(3), 239–243.

Hubbard, C., McNamara, J. T., Azumaya, C., Patel, M. S., & Zimmer, J. (2012). The hyaluronan synthase catalyzes the synthesis and membrane translocation of hyaluronan. *Journal of Molecular Biology*, *418*(1–2), 21–31.

Im, J.-H., Song, J.-M., Kang, J.-H., & Kang, D.-J. (2009). Optimization of medium components for high-molecular-weight hyaluronic acid production by *Streptococcus* sp. ID9102 via a statistical approach. *Journal of Industrial Microbiology & Biotechnology*, *36*(11), 1337–1344.

Jeong, E., Shim, W. Y., & Kim, J. H. (2014). Metabolic engineering of *Pichia pastoris* for production of hyaluronic acid with high molecular weight. *Journal of Biotechnology*, *185*, 28–36.

Jin, P., Kang, Z., Yuan, P., Du, G., & Chen, J. (2016). Production of specific-molecular-weight hyaluronan by metabolically engineered *Bacillus subtilis* 168. *Metabolic Engineering*, *35*, 21–30.

Kawai, F., Hara, H., Takamatsu, H., Watabe, K., & Matsumoto, K. (2006). Cardiolipin enrichment in spore membranes and its involvement in germination of *Bacillus subtilis* Marburg. *Genes & Genetic Systems*, *81*(2), 69–76.

Kawai, F., Shoda, M., Harashima, R., Sadaie, Y., Hara, H., & Matsumoto, K. (2004). Cardiolipin domains in *Bacillus subtilis* Marburg membranes. *Journal of Bacteriology*, *186*(5), 1475–1483.

Kennard, O. (1985). Structural studies of DNA fragments: The G·T wobble base pair in A, B and Z DNA; the G·A base pair in B-DNA. *Journal of Biomolecular Structure and Dynamics*, *3*(2), 205–226.

Kim, J.-H., Yoo, S.-J., Oh, D.-K., Kweon, Y.-G., Park, D.-W., Lee, C.-H., & Gil, G.-H. (1996). Selection of a *Streptococcus equi* mutant and optimization of culture conditions for the production of high molecular weight hyaluronic acid. *Enzyme and Microbial Technology*, *19*(6), 440–445.

Kobayashi, K., Ehrlich, S. D., Albertini, A., Amati, G., Andersen, K. K., Arnaud, M., ... Ogasawara, N. (2003). Essential *Bacillus subtilis* genes. *Proceedings of the National Academy of Sciences*, *100*(8), 4678–4683.

Kumari, K., Baggenstoss, B. A., Parker, A. L., & Weigel, P. H. (2006). Mutation of two intramembrane polar residues conserved within the hyaluronan synthase family alters hyaluronan product size. *Journal of Biological Chemistry*, *281*(17), 11755–11760.

Kumari, K., & Weigel, P. H. (1997). Molecular cloning, expression, and characterization of the authentic hyaluronan synthase from group C *Streptococcus equisimilis*. *Journal of Biological Chemistry*, *272*(51), 32539–32546.

Larson, M. H., Gilbert, L. A., Wang, X., Lim, W. A., Weissman, J. S., & Qi, L. S. (2013). CRISPR interference (CRISPRi) for sequence-specific control of gene expression. *Nature Protocols*, *8*(11), 2180–2196.

Liu, L., Liu, Y., Li, J., Du, G., & Chen, J. (2011). Microbial production of hyaluronic acid: Current state, challenges, and perspectives. *Microbial Cell Factories*, *10*(1), 99.

Lopez, C. S., Alice, A. F., Heras, H., Rivas, E. A., & Sanchez-Rivas, C. (2006). Role of anionic phospholipids in the adaptation of *Bacillus subtilis* to high salinity. *Microbiology*, *152*(3), 605–616.

MacGilvray, M. E., Lapek, J. D., Jr, Friedman, A. E., & Quivey, R. G., Jr. (2012). Cardiolipin biosynthesis in *Streptococcus mutans* is regulated in response to external pH. *Microbiology*, *158*(8), 2133–2143.

Mamat, U., Wilke, K., Bramhill, D., Schromm, A. B., Lindner, B., Kohl, T. A., ... Head, S. R. (2015). Detoxifying *Escherichia coli* for endotoxin-free production of recombinant proteins. *Microbial Cell Factories*, *14*(1), 57.

Mao, Z., Shin, H.-D., & Chen, R. (2009). A recombinant *E. coli* bioprocess for hyaluronan synthesis. *Applied Microbiology and Biotechnology*, *84*(1), 63–69.

Medina, A., Lin, J., & Weigel, P. (2012). Hyaluronan synthase mediates dye translocation across liposomal membranes. *BMC Biochemistry*, *13*(1), 2.

Mileykovskaya, E., & Dowhan, W. (2000). Visualization of phospholipid domains in *Escherichia coli* by using the cardiolipin-specific fluorescent dye 10-N-nonyl acridine orange. *Journal of Bacteriology*, *182*(4), 1172–1175.

Monahan, L. G., Hajduk, I. V., Blaber, S. P., Charles, I. G., & Harry, E. J. (2014). Coordinating bacterial cell division with nutrient availability: A role for glycolysis. *MBio*, *5*(3), e00935–e00914.

Monterroso, B., Ahijado-Guzmán, R., Reija, B., Alfonso, C., Zorrilla, S., Minton, A. P., & Rivas, G. (2012). Mg^{2+}-linked self-assembly of FtsZ in the presence of GTP or a GTP analog involves the concerted formation of a narrow size distribution of oligomeric species. *Biochemistry*, *51*(22), 4541.

Nguyen, H., Phan, T., & Schumann, W. (2007). Expression vectors for the rapid purification of recombinant proteins in *Bacillus subtilis*. *Current Microbiology*, *55*(2), 89–93.

Nishibori, A., Kusaka, J., Hara, H., Umeda, M., & Matsumoto, K. (2005). Phosphatidylethanolamine domains and localization of phospholipid synthases in *Bacillus subtilis* membranes. *Journal of Bacteriology*, *187*(6), 2163–2174.

Nudler, E., Kashlev, M., Nikiforov, V., & Goldfarb, A. (1995). Coupling between transcription termination and RNA polymerase inchworming. *Cell*, *81*(3), 351–357.

O'Regan, M., Martini, I., Crescenzi, F., De Luca, C., & Lansing, M. (1994). Molecular mechanisms and genetics of hyaluronan biosynthesis. *International Journal of Biological Macromolecules*, *16*(6), 283–286.

Ouskova, G., Spellerberg, B., & Prehm, P. (2004). Hyaluronan release from *Streptococcus pyogenes*: Export by an ABC transporter. *Glycobiology*, *14*(10), 931–938.

Pagano, A., Castelnuovo, M., Tortelli, F., Ferrari, R., Dieci, G., & Cancedda, R. (2007). New small nuclear RNA gene-like transcriptional units as sources of regulatory transcripts. *PLoS Genet*, *3*(2), e1.

Percy, M. G., & Gründling, A. (2014). Lipoteichoic acid synthesis and function in gram-positive bacteria. *Annual Review of Microbiology*, *68*, 81–100.

Phan, T. T. P., Nguyen, H. D., & Schumann, W. (2012). Development of a strong intracellular expression system for *Bacillus subtilis* by optimizing promoter elements. *Journal of Biotechnology*, *157*(1), 167–172.

Prasad, S., Jayaraman, G., & Ramachandran, K. B. (2010). Hyaluronic acid production is enhanced by the additional co-expression of UDP-glucose pyrophosphorylase in *Lactococcus lactis*. *Applied Microbiology and Biotechnology*, *86*(1), 273–283.

Pullman-Mooar, S., Mooar, P., Sieck, M., Clayburne, G., & Schumacher, H. R. (2002). Are there distinctive inflammatory flares after hylan g-f 20 intraarticular injections? *The Journal of Rheumatology*, *29*(12), 2611–2614.

Qi Lei, S., Larson Matthew, H., Gilbert Luke, A., Doudna Jennifer, A., Weissman Jonathan, S., Arkin Adam, P., & Lim Wendell, A. (2013). Repurposing CRISPR as an RNA-guided platform for sequence-specific control of gene expression. *Cell*, *152*(5), 1173–1183.

Rosch, J. W., Hsu, F. F., & Caparon, M. G. (2007). Anionic lipids enriched at the ExPortal of *Streptococcus pyogenes*. *Journal of Bacteriology*, *189*(3), 801–806.

Salzberg, L. I., & Helmann, J. D. (2008). Phenotypic and transcriptomic characterization of *Bacillus subtilis* mutants with grossly altered membrane composition. *Journal of Bacteriology*, *190*(23), 7797–7807.

Sambrook, J., & Russell, D. (2001). *Molecular cloning: A laboratory manual*. Harbor, NY: Cold Spring Harbor Laboratory Press.

Schallmey, M., Singh, A., & Ward, O. P. (2004). Developments in the use of *Bacillus* species for industrial production. *Canadian Journal of Microbiology*, *50*(1), 1–17.

Schneider, C. A., Rasband, W. S., & Eliceiri, K. W. (2012). NIH Image to ImageJ: 25 years of image analysis. *Nature Methods*, *9*(7), 671–675.

Shiomi, D., & Margolin, W. (2007). A sweet sensor for size-conscious bacteria. *Cell*, *130*(2), 216–218.

Soldo, B., Lazarevic, V., Pagni, M., & Karamata, D. (1999). Teichuronic acid operon of *Bacillus subtilis* 168. *Molecular Microbiology*, *31*(3), 795–805.

Tlapak-Simmons, V. L., Baggenstoss, B. A., Clyne, T., & Weigel, P. H. (1999). Purification and lipid dependence of the recombinant hyaluronan synthases from *Streptococcus pyogenes* and *Streptococcus equisimilis*. *Journal of Biological Chemistry*, *274*(7), 4239–4245.

Tlapak-Simmons, V. L., Baron, C. A., & Weigel, P. H. (2004). Characterization of the purified hyaluronan synthase from *Streptococcus equisimilis*. *Biochemistry*, *43*(28), 9234–9242.

Tlapak-Simmons, V. L., Kempner, E. S., Baggenstoss, B. A., & Weigel, P. H. (1998). The active streptococcal hyaluronan synthases (HASs) contain a single HAS monomer and multiple cardiolipin molecules. *Journal of Biological Chemistry*, *273*(40), 26100–26109.

Triscott, M. X., & van de Rijn, I. (1986). Solubilization of hyaluronic acid synthetic activity from streptococci and its activation with phospholipids. *Journal of Biological Chemistry*, *261*(13), 6004–6009.

Vázquez, J. A., Montemayor, M. I., Fraguas, J., & Murado, M. A. (2010). Hyaluronic acid production by *Streptococcus zooepidemicus* in marine by-products media from mussel processing wastewaters and tuna peptone viscera. *Microbial Cell Factories*, *9*(1), 1–10.

Weigel, P. H. (2002). Functional characteristics and catalytic mechanisms of the bacterial hyaluronan synthases. *IUBMB Life*, *54*(4), 201–211.

Weigel, P. H., & Baggenstoss, B. A. (2012). Hyaluronan synthase polymerizing activity and control of product size are discrete enzyme

functions that can be uncoupled by mutagenesis of conserved cysteines. *Glycobiology*, *22*(10), 1302–1310.

Weigel, P. H., & DeAngelis, P. L. (2007). Hyaluronan synthases: A decade-plus of novel glycosyltransferases. *Journal of Biological Chemistry*, *282*(51), 36777–36781.

Westbrook, A. W., Moo-Young, M., & Chou, C. P. (2016). Development of a CRISPR-Cas9 toolkit for comprehensive engineering of *Bacillus subtilis*. *Applied and Environmental Microbiology*, *82*(16), 4876–4895.

Widner, B., Behr, R., Von Dollen, S., Tang, M., Heu, T., Sloma, A., . . . Brown, S. (2005). Hyaluronic acid production in *Bacillus subtilis*. *Applied and Environmental Microbiology*, *71*(7), 3747–3752.

Wolf, M., Geczi, A., Simon, O., & Borriss, R. (1995). Genes encoding xylan and β-glucan hydrolysing enzymes in *Bacillus subtilis*: characterization, mapping and construction of strains deficient in lichenase, cellulase and xylanase. *Microbiology*, *141*(2), 281–290.

Yoshimura, T., Shibata, N., Hamano, Y., & Yamanaka, K. (2015). Heterologous production of hyaluronic acid in an ε-poly-L-lysine producer, *Streptomyces albulus*. *Applied and Environmental Microbiology*, *81*(11), 3631–3640.

Yu, H., & Stephanopoulos, G. (2008). Metabolic engineering of *Escherichia coli* for biosynthesis of hyaluronic acid. *Metabolic Engineering*, *10*(1), 24–32.

SUPPORTING INFORMATION

Additional Supporting Information may be found online in the supporting information tab for this article.

How to cite this article: Westbrook AW, Ren X, Moo-Young M, Chou CP. Engineering of cell membrane to enhance heterologous production of hyaluronic acid in *Bacillus subtilis*. *Biotechnology and Bioengineering*. 2018;115:216–231. https://doi.org/10.1002/bit.26459